Articles

9-Hydroxyazafluorenes and Their Use in Thrombin Inhibitors

Kenneth J. Stauffer,*,† Peter D. Williams,† Harold G. Selnick,† Philippe G. Nantermet,† Christina L. Newton,†,▽ Carl F. Homnick,† Matthew M. Zrada,† S. Dale Lewis,‡ Bobby J. Lucas,‡ Julie A. Krueger,‡ Beth L. Pietrak,‡ Elizabeth A. Lyle,§ Rominder Singh,∥ Cynthia Miller-Stein,∥ Rebecca B. White,∥ Bradley Wong,∥ Audrey A. Wallace,§ Gary R. Sitko,§ Jacquelyn J. Cook,§ Marie A. Holahan,§ Maria Stranieri-Michener,§ Yvonne M. Leonard,§ Joseph J. Lynch, Jr.,§ Daniel R. McMasters,⊥ and Youwei Yan⊗

Departments of Medicinal Chemistry, Biological Chemistry, Pharmacology, Drug Metabolism, and Molecular Systems, Merck Research Laboratories, West Point, Pennsylvania 19486

Received July 20, 2004

Optimization of a previously reported thrombin inhibitor, 9-hydroxy-9-fluorenylcarbonyl-L-prolyl-*trans*-4-aminocyclohexylmethylamide (**1**), by replacing the aminocyclohexyl P1 group provided a new lead structure, 9-hydroxy-9-fluorenylcarbonyl-L-prolyl-2-aminomethyl-5-chlorobenzylamide (**2**), with improved potency (K_i = 0.49 nM for human thrombin, 2× APTT = 0.37 μM in human plasma) and pharmacokinetic properties (F = 39%, iv $T_{1/2}$ = 13 h in dogs). An effective strategy for reducing plasma protein binding of **2** and improving efficacy in an in vivo thrombosis model in rats was to replace the lipophilic fluorenyl group in P3 with an azafluorenyl group. Systematic investigation of all possible azafluorenyl P3 isomers and azafluorenyl-*N*-oxide analogues of **2** led to the identification of an optimal compound, 3-aza-9-hydroxyfluoren-9(*R*)-ylcarbonyl-L-prolyl-2-aminomethyl-5-chlorobenzylamide (**19b**), with high potency (K_i = 0.40 nM, 2× APTT = 0.18 μM), excellent pharmacokinetic properties (F = 55%, $T_{1/2}$ = 14 h in dogs), and complete efficacy in the in vivo thrombosis model in rats (inhibition of $FeCl_3$-induced vessel occlusions in six of six rats receiving an intravenous infusion of 10 μg/kg/min of **19b**). The stereochemistry of the azafluorenyl group in **19b** was determined by X-ray crystallographic analysis of its *N*-oxide derivative (**23b**) bound in the active site of human thrombin.

Introduction

The serine protease, thrombin, is a critical enzyme in the coagulation cascade. The primary components of a vascular thrombus, activated platelets and fibrin, are both produced by mechanisms involving proteolysis catalyzed by thrombin. Inhibitors of thrombin have long been recognized as potential therapeutic agents for the treatment of a variety of thrombotic disorders, and indeed, intravenous and oral thrombin inhibitors have recently progressed through human clinical trials and reached the marketplace.[1,2] Our goal has been to identify a once a day oral thrombin inhibitor with predictable pharmacokinetics and no clinically meaningful food or drug interactions. Such a compound would offer significant advantages over the two most widely employed antithrombotic drugs, low molecular weight heparin (the requirement for parenteral administration precludes its use on a chronic basis) and warfarin (frequent patient monitoring is required because of its slow onset of action, variable interpatient dose−response, and significant food and drug interactions).

Several years ago we reported the optimization of a series of thrombin inhibitors containing an L-prolyl-*trans*-4-aminocyclohexylmethylamide P2−P1 scaffold, using parallel solid-phase synthesis methods to vary the P3 portion of the molecule.[3] An interesting inhibitor which incorporates a 9-hydroxyfluorenyl group in P3 was identified from this work (**1**, see Figure 1). In an isolated enzyme assay **1** inhibited human thrombin with a K_i value of 1.5 nM and **1** had good selectivity for inhibiting thrombin versus a panel of other human serine proteases (K_i = 860 nM trypsin; $K_i \geq 20$ μM for plasmin, tPA, activated protein C, plasma kallikrein, and chymotrypsin). In functional assays, **1** inhibited coagulation of human plasma triggered by the intrinsic pathway with a doubling of the activated partial thromboplastin time (2× APTT) at a concentration of 0.85 μM, and in an arterial thrombosis model in rats, an intravenous infusion of 10 μg/kg/min of **1** inhibited $FeCl_3$-induced vessel occlusion in six of six animals. The 9-hydroxyfluorenyl group also engendered **1** with superior pharmacokinetic properties compared to numerous P3 variants in this P2−P1 structural series (F = 74%,

* To whom correspondence should be addressed. Phone: 215-652-5264, fax 215-652-3971, e-mail ken_stauffer@merck.com.
† Medicinal Chemistry.
‡ Biological Chemistry.
§ Pharmacology.
∥ Drug Metabolism.
⊥ Molecular Systems.
⊗ Structural Biology.
▽ Deceased June 29, 2001.

10.1021/jm049423s CCC: $30.25
Published on Web 02/24/2005

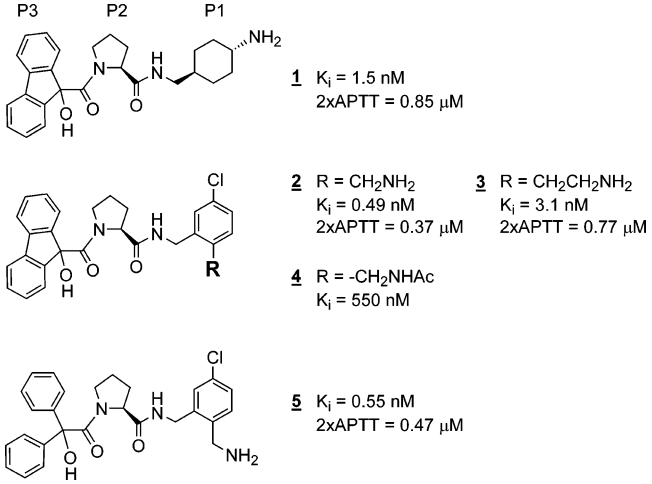

Figure 1.

iv $T_{1/2}$ = 2 h in dogs; F = 39%, iv $T_{1/2}$ = 4 h in cynomologus monkeys).

X-ray crystallographic analysis of **1** bound to the active site of human thrombin showed one of the benzene rings of the P3 hydroxyfluorenyl group to be binding in the hydrophobic S3 pocket of the enzyme, the other benzene ring contacting the hydrophobic residues Tyr-60A and Trp-60D contained in the loop which also contacts the P2 proline, the hydroxyl group hydrogen bonding to the carbonyl of Gly-216, and the P1 aminocyclohexyl moiety binding in the S1 pocket of the enzyme with the amino group interacting with Asp-189.

Having optimized the P3−P2 portion of the molecule with the 9-hydroxyfluorenyl-prolyl moiety, we began to screen new P1 group analogues of **1** for improved performance. Our laboratories were also developing new P1 structures based on the previously reported 2,5-dichlorobenzylamide template,[4] replacing the chlorine at position 2 with a variety of new substituents. An interesting finding from this work was that an aminomethyl or aminoethyl group at position 2 brought about a large increase in binding potency by forming a salt bridge with a surface glutamate on the enzyme as well as making several other inter- and intramolecular hydrogen bonds.[5] Incorporation of these new P1 groups into the 9-hydroxyfluorenyl-prolyl P3−P2 scaffold gave **2** and **3** (Figure 1). The aminomethyl analogue **2** displayed superior potency compared to the aminoethyl analogue **3** and **1** in both the isolated enzyme and the 2× APTT assays. Both **2** and **3** exhibited excellent pharmacokinetic properties in dogs (**2**, F = 39%; iv $T_{1/2}$ = 13 h; **3**, F = 39%; iv $T_{1/2}$ = 14 h) with plasma half-lives improved by 6-fold compared to **1**.

The free P1 amino group and the P3 fluorenyl group in **2** were found to be important structural features for obtaining favorable pharmacokinetic properties. For example, replacing the basic P1 amino group with an acetamido group (**4**, Figure 1), in addition to reducing potency, brought about a dramatic reduction of exposure in the systemic circulation and plasma half-life after an oral dose of 1 mg/kg in dogs (AUC = 0.04 μM·h, $T_{1/2}$ = 0.48 h) compared to **2** (AUC = 32 μM·h, $T_{1/2}$ = 13 h). Likewise, a simple alteration of the P3 group involving opening of the tricyclic fluorenyl ring (**5**, Figure 1), while having little effect on potency, also reduced systemic exposure and plasma half-life after a 1 mg/kg oral dose in dogs (AUC = 13 μM·h, $T_{1/2}$ = 4.2 h) compared to **2**.

Both **2** and **3** showed reduced efficacy for inhibiting $FeCl_3$-induced thrombosis in rats compared to **1**. While an intravenous infusion of 10 μg/kg/min of **1** was fully efficacious in six rats (0/6 occlusions), the same dose of **2** and **3** resulted in vessel occlusions in 4/5 and 6/6 animals, respectively. Possibly contributing to the poor efficacy was the fact that both **2** and **3** were more highly bound to blood plasma proteins (**2**, 1% free in human plasma, 9% free in rat plasma; **3**, 3% free in human plasma, 15% free in rat plasma) than **1** (8% free in human plasma, 27% free in rat plasma). From our previous work, we were aware that reducing inhibitor lipophilicity can lessen plasma protein binding and improve efficacy in both the 2× APTT assay and the $FeCl_3$-induced thrombosis assay in rats.[6] One way to accomplish this in the present series was to replace the fluorenyl ring in P3 with an azafluorenyl ring. It was thought that this type of modification would reduce lipophilicity while maintaining, as much as possible, the structural features important for good intrinsic potency and good pharmacokinetic properties. Additionally, since it is well-known that pyridine derivatives are capable of being metabolized to their corresponding *N*-oxides, analogues containing an azafluorenyl-*N*-oxide group in P3 were also of interest. Herein we detail the synthesis and biological properties of analogues of lead compound **2** which contain all possible isomers of 9-hydroxyazafluorene and the corresponding *N*-oxides in the P3 position.

Synthetic Chemistry

The Boc protected prolylchlorobenzylamide derivative **7** served as a key common intermediate for the compounds in Table 1. Compound **7** was prepared in a straightforward fashion using 2-(*tert*-butyloxycarbonylaminomethyl)-5-chlorobenzylamine **6**[7] as depicted in eq 1 of Scheme 1. Acylation of **7** with 9-hydroxyfluorene-9-carboxylic acid using standard peptide coupling conditions followed by removal of the Boc protecting group under acidic conditions gave **2** in very good overall yield.

Synthesis of azafluorenyl P3 analogues of **2** was envisioned as utilizing azafluorenones as key intermediates. The keto group of the azafluorenone could in principle be converted to a cyanohydrin and then hydrolyzed to a hydroxy acid for coupling to amine **7**. Several methods for preparing azafluorenones have been reported,[8] and the method which proved to be the best suited for our purposes was that which utilizes an intramolecular Friedel−Crafts reaction of a pyridine substrate containing adjacent carboxy and phenyl substituents. Synthesis of the 4-azafluorene-containing inhibitors, **20a**,**b** and **24a**,**b**, is shown in eq 2 of Scheme 1. 2-Chloro-3-cyanopyridine underwent efficient Suzuki coupling with phenylboronic acid followed by acid hydrolysis to give the Friedel−Crafts substrate **8**. Hot polyphosphoric acid induced efficient cyclization of **8** to 4-azafluorenone **9**. A more direct method of synthesizing **9** was also developed which involves a one-step oxidative ring contraction of 7,8-benzoquinoline using basic permanganate, reaction conditions analogous to what has

Table 1.

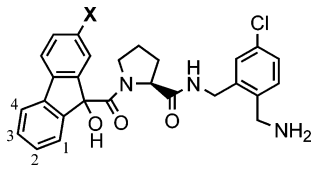

	position of aza or aza-N-oxide substitution	X	thrombin K_i (nM)[a]	2× APTT (μM)[a]	plasma protein binding (% free) human	plasma protein binding (% free) rat	in vivo rat thrombosis model occlusions	dog pharmacokinetics[b] 1 mg/kg po AUC (μM·h)	dog pharmacokinetics[b] 1 mg/kg po $T_{1/2}$ (h)
2	-	H	0.49	0.37	1	9	4/5	32	13[c]
17a	1N	H	3.3	0.50	7	10	3/6	22	6.0
17b	1N	H	0.20	0.13	9	32	0/3	2.8	2.5
18a	2N	H	3.2	0.94	13	34	0/5	12	2.5
18b	2N	H	0.30	0.12	27	30	0/6	24	10
19a	3N	H	2.0	0.29	22	18	3/5	2.4	2.0
19b	3N	H	0.40	0.18	8	20	0/6	28	14[c]
20a	4N	H	1.4	0.23	12	13	0/6	14	6.1
20b	4N	H	0.78	0.17	12	36	0/5	48	5.5[c]
21a	1N−O	H	140	-	-	-	-	-	-
21b	1N−O	H	0.25	0.085	35	55	0/3	0.029	1.3
22a	2N−O	H	37	-	-	-	-	-	-
22b	2N−O	H	0.98	0.13	59	70	0/6	0.28	1.8
23a	3N−O	H	4.4	0.71	-	-	-	-	-
23b	3N−O	H	0.77	0.19	16	41	1/5	1.5	1.8
24a	4N−O	H	3.3	0.43	-	-	-	-	-
24b	4N−O	H	2.1	0.27	56	42	0/6	2.9	5.7[c]
25a	4N	Cl	1.1	0.22	6	6	1/6	7.0	3.1
25b	4N	Cl	0.042	0.13	11	18	0/6	1.7	3.8

[a] The reported thrombin K_i values and 2× APTT values are from one or two determinations; typical standard error in these assays is ±20%. [b] Compounds were dosed as TFA salts in 1% methocel suspension in male beagle dogs ($n = 2$); typical standard error in the measurement of AUC is ±20%. [c] Plasma half-life after a 1 mg/kg iv dose in male beagle dogs ($n = 2$).

Scheme 1[a]

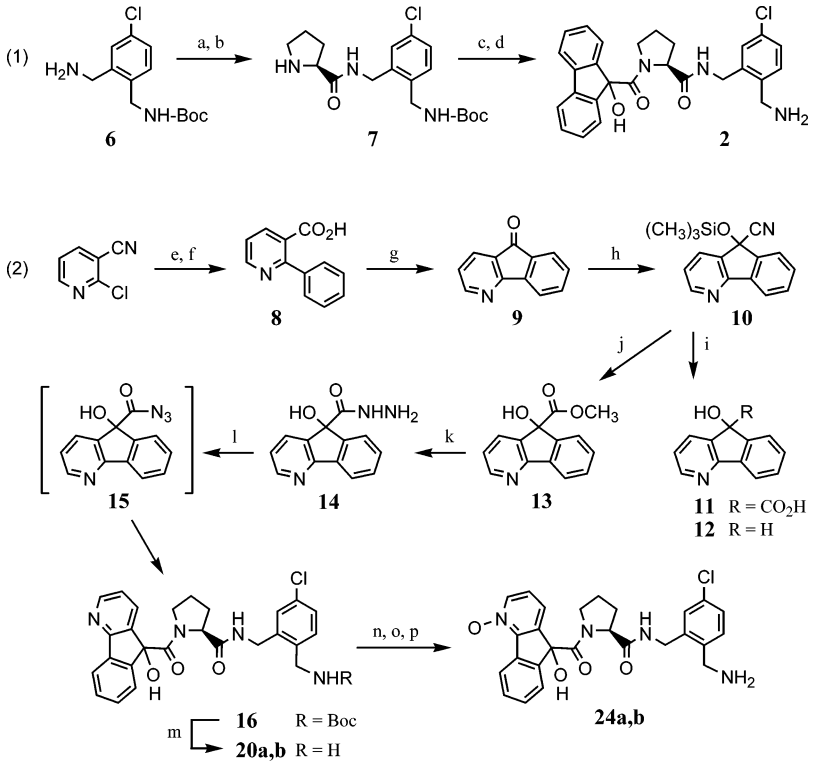

[a] Reagents and conditions: a. Fmoc-L-proline, EDC, HOBT (94%); b. piperidine, DMF (90%); c. 9-hydroxy-9-fluorenecarboxylic acid, EDC, HOBT (90%); d. HCl(g), EtOAc (89%); e. $PhB(OH)_2$, $Pd(PPh_3)_4$, K_2CO_3 (94%); f. concentrated HCl, reflux (99%); g. polyphosphoric acid, 190 °C (92%); h. $(CH_3)_3SiCN$, ZnI_2, reflux; i. concentrated HCl, HOAc (20%); j. HCl(g), MeOH (70%); k. hydrazine, 50 °C (85%); l. amyl nitrite, **7**, −20 °C (85%); m. TFA, CH_2Cl_2, chromatographic separation of diasteromers (36%); n. $(^tBuO_2C)_2O$ (91%); o. MCPBA, CH_2Cl_2 (44%); p. TFA, CH_2Cl_2 (95%).

been reported for the preparation of 4,5-diazafluorenone.[9] 4-Azafluorenone **9** was readily converted to trimethylsilyl cyanohydrin **10** upon heating in trimethylsilyl cyanide with zinc iodide catalysis.[10] Hydrolysis[11] of **10** to the corresponding hydroxy acid **11**, however, proved to be problematic due to competing decarboxy-

lation to alcohol **12**. Additionally, the coupling of **11** to proline derivative **7** under a variety of conditions produced the desired product **16** in very low yields (<5%) due to competitive decarboxylation of **11** during the reaction. While the parent, 9-hydroxyfluorene-9-carboxylic acid, is chemically stable and well-behaved in peptide coupling reactions, the electron-withdrawing effect of the nitrogen in the 4-azafluorenyl analogue **11** was found to vastly increase the propensity for decarboxylation, making peptide couplings extremely difficult. At the time this work was ongoing, a report on the preparation of 9-amino-4,5-di-azafluorenyl-9-carboxamide peptide derivatives appeared.[12] The coupling procedure in this report avoided the intermediacy of a carboxylic acid and instead employed a hydrazide which was converted to an acyl azide as the reactive acylating species. A similar approach was adopted in our work and resulted in greatly improved yields. The treatment of trimethylsilyl cyanohydrin **10** with HCl gas in methanol provided hydroxy ester **13**, and heating **13** with excess hydrazine produced hydrazide **14**. Treatment of **14** with amyl nitrite at low temperature produced acyl azide **15**, the presence of which could be detected by LC-MS, and **15** slowly acylated **7** at low temperature to provide the desired coupling product **16** in 85% isolated yield. Byproducts observed in this reaction were ketone **9** and alcohol **12** which presumably had arisen from Curtius rearrangement and hydrolysis/decarboxylation reactions of **15**, respectively. Removal of the Boc group in **16** followed by chromatographic separation provided the individual 4-azafluorenyl P3 diastereomers **20a** and **20b**. A portion of each diastereomer was reprotected with di-*tert*-butyl dicarbonate, oxidized with MCPBA, and then deprotected with acid to give the corresponding *N*-oxide derivatives **24a** and **24b**.

The remainder of the compounds in Table 1 were prepared in a manner analogous to that shown in eq 2 of Scheme 1, starting with the different isomers of **8**. The carboxylic acid obtained from methyl 4-phenylpyridine-3-carboxylate,[13] was employed as the Friedel–Crafts substrate for the preparation of compounds in the 2-azafluorene series (**18a**,**b** and **22a**,**b**). Methyl 3-bromopyridine-2-carboxylate and methyl 3-bromopyridine-4-carboxylate, prepared by the method of Epsztajn et al.,[14] underwent efficient Suzuki coupling with phenylboronic acid, and following ester group hydrolysis, gave the appropriate Freidel-Crafts substrates for the preparation of compounds in the 1-azafluorene series (**17a**,**b** and **21a**,**b**), and 3-azafluorene series (**19a**,**b** and **23a**,**b**), respectively. 7-Chloro-4-azafluorenone was prepared by the method of DuPriest et al.[15] and was used to obtain **25a** and **25b**.

Yields in the acyl azide coupling reaction with proline derivative **7** were found to be substrate dependent. Higher yields were obtained with the 1- and 4-azafluorenyl isomers (62% and 85%, respectively), and lower yields resulted with the 2- and 3-azafluorenyl isomers (8% and 13%, respectively). Yields with the 2- and 3-azafluorenyl isomers, however, were substantially improved by adding HOAT to the acyl azide to make an active ester,[16] prior to the addition of proline coupling partner **7** (30% and 44% yields, respectively, in the presence of HOAT).

Compounds **17a**,**b**–**20a**,**b**, and **25a**,**b** in Table 1 were prepared as mixtures of P3 diastereomers. For each mixture, chromatographic conditions were identified which provided the individual diastereomers in pure form. The diastereomers with the 3-azafluorenyl P3 group, **19a**,**b**, although separable, were very closely eluting under a variety of chromatographic conditions, thus making isolation of larger quantities difficult. A more efficient separation was possible at the Boc-protected precursor stage. Alternatively, efficient separation of enantiomers at the hydroxy ester stage (the 3-azafluorene isomer of **13**) was accomplished using HPLC on a chiral stationary phase, and further processing of the (−) enantiomer provided access to larger quantities of **19b**.

Biological Assays

Inhibition constants (K_i values) were determined for test compounds in an assay using human derived thrombin, trypsin, urokinase, plasmin, kallikrein, t-PA and chymotrypsin with the corresponding fluorescent or chromogenic substrate under steady state conditions as previously described.[17] The concentration of test compound required to double the activated partial thromboplastin time in human plasma, the 2× APTT value, was determined under conditions involving a 3-fold dilution of human plasma as previously reported.[18] The antithrombotic activities of intravenously administered test compounds were determined in an anesthetized rat model of topical $FeCl_3$-induced arterial thrombosis.[19] Test compounds were administered by intravenous infusion at a dose of 10 μg/kg/min for 180 min, $FeCl_3$ was applied to the carotid artery at 120 min post dose, and carotid artery blood flow was monitored for 60 min. Results are expressed as number of animals which had occluded vessels (n = 5 or 6). For plasma pharmacokinetic assays, amorphous TFA salts of test compounds were dosed orally in 1% methocel solution to beagle dogs (n = 2) at 1 mg/kg. Blood samples were obtained over 8 h postdose, and a final blood sample was taken at 24 h. At each time point, test compound was isolated from the plasma fraction by solid-phase extraction and quantified by LC-MS/MS against a standard curve. Area under the curve (AUC) and plasma half-life ($T_{1/2}$) were determined from analysis of the concentration versus time curve. Plasma protein binding was determined as previously described.[6] Standard error in the measurement of thrombin K_i values, 2× APTT values, and oral AUC values is ±20%.

Results and Discussion

Assay results for the diastereomeric pairs of each of the four azafluorenyl positional isomers and selected *N*-oxide derivatives are collected in Table 1. Comparing the intrinsic potency (K_i vs human thrombin) of the aza analogues **17a**,**b**–**20a**,**b** to lead compound **2**, it is seen that introduction of nitrogen into the fluorenyl ring system is generally well-tolerated, with potencies ranging from 6-fold less potent (**17a**, **18a**) to 2.5-fold more potent (**17b**) than **2**. The difference in potency between the two diastereomers for each of the four positional isomers progressively decreased as the nitrogen was moved around the fluorenyl ring from the 1-position (**17a/17b**, difference of 17-fold) to the 4-position (**20a/**

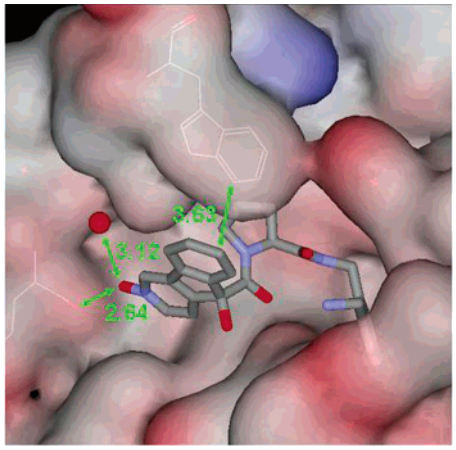

Figure 2. Active site region from the X-ray structure of the **23b**−thrombin complex highlighting several interactions of the azafluorenyl *N*-oxide P3 moiety with the enzyme.

20b, difference of 1.8-fold). Comparing the more potent diastereomers from each pair of positional isomers, **17b-20b**, it is seen that potency progressively increased as the nitrogen was moved around the fluorenyl ring from the 4-position (**20b**, $K_i = 0.78$ nM) to the 1-position (**17b**, $K_i = 0.20$ nM). Conversion of each of the azafluorenyl diastereomers **17a**,**b**−**20a**,**b** to its corresponding *N*-oxide derivative, **21a**,**b**−**24a**,**b**, resulted in a small loss of potency (1.3-fold to 3.3-fold) except for azafluorenes **17a** and **18a**, where the loss in potency was larger (42-fold and 12-fold loss of potency for *N*-oxides **21a** and **22a**, respectively). Addition of a chlorine at the 7-position of the 4-azafluorenyl ring produced a very potent inhibitor with diastereomer **25b**. For all the compounds in Table 1, excellent selectivity for inhibiting thrombin vs the related serine protease, trypsin, was observed, with selectivity ratios ranging from 1000-fold to 7000-fold. Compound **25b** displayed the greatest absolute potency for trypsin in the group, with a K_i value of 300 nM.

The structure of compound **23b** bound in the active site of human thrombin was determined by X-ray crystallographic analysis (see Figure 2). The positioning of the P1 aminomethyl chlorobenzyl group in the S1 pocket was found to be virtually identical to that previously observed for a thrombin inhibitor utilizing a pyridinone P2 template,[5] with the aminomethyl group in **23b** forming a salt bridge with Glu-192 as well as being within hydrogen-bonding distance of four additional H-bond acceptors: the Gly-216 carbonyl oxygen, the proline carbonyl oxygen, the carbonyl oxygen of the azafluorenyl-9-carboxamide, and a crystallographically resolved water molecule. We were somewhat surprised, however, to find that **23b**, the more potent of the two diastereomerically related 3-azafluorenyl-*N*-oxides **23a** and **23b**, has the *R* configuration in P3, i.e., the isomer which has the aza-*N*-oxide ring pointed in toward the S3 pocket. Prior to determination of this structure, visual inspection of the fluorenyl group in the X-ray structure of lead compound **1** bound in the thrombin active site led us to speculate that the *R*-isomers of the position 1-, 2-, and 3-azafluorenyl-*N*-oxides might bind less tightly than the corresponding *S*-isomers because of unfavorable steric interactions of the *N*-oxide group with the enzyme. The structure of **23b** shows the *N*-oxide oxygen to be located 2.6 Å from the backbone carbonyl oxygen of Glu-97A which is presumably a destabilizing electrostatic interaction. However, a crystallographically resolved water molecule, shown as a red sphere in Figure 2, is within hydrogen bonding distance (3.1 Å) of the aza-fluorenyl-*N*-oxide oxygen and may help to stabilize positioning of the *N*-oxide group in the S3 pocket. This water molecule is also within hydrogen bonding distance to the carbonyl oxygen of Trp-96 (2.5 Å) and the phenolic hydroxyl group of Tyr-60A (2.8 Å). Also, there is an aromatic ring edge-to-face interaction involving the indole side chain of Trp-60D (edge) and the benzenoid ring portion of the tricyclic azafluorenyl-*N*-oxide (face). These two rings are separated by a distance of approximately 3.6 Å as indicated in Figure 2. Of the two diastereomers **23a** and **23b**, we speculate that the electropositive edge of the Trp-60D side chain would engage in a more favorable electrostatic interaction with the π-face of the more electron rich benzenoid ring portion of the tricyclic azafluorenyl-*N*-oxide ring system in diastereomer **23b** than it would with the π-face of the more electron deficient *N*-oxide ring portion of the azafluorenyl-*N*-oxide group upon binding of diastereomer **23a**. Crystal structures of other positional azafluorenyl-*N*-oxide isomers are needed to more fully understand the relationship between inhibitor P3 interactions with the enzyme and binding potency in this series of compounds.

Compared to **2**, azafluorenyl analogues **17a**,**b**−**20a**,**b** all showed reduced binding to plasma proteins in both human and rat plasma. Human plasma protein binding was particularly high with **2**, and as predicted, the free fraction was significantly increased with the introduction of nitrogen into the fluorenyl ring. Conversion of the azafluorenyl analogues to their corresponding *N*-oxides increased the free fraction to an even greater extent. The 4-azafluorenyl analogue **20b** and its corresponding *N*-oxide **24b** illustrate this point, with 10-fold and 50-fold increases in the free fraction in human plasma, respectively, compared to **2**. Reducing human plasma protein binding had beneficial effects on efficacy in the 2× APTT assay. For example, although the intrinsic potencies of **20b**, **22b**, **23b**, **24b**, and **25a** are all less than that of **2**, the former are all more potent than **2** in the 2× APTT assay. Azafluorenes **17a**,**b**−**20a**,**b** and *N*-oxides **21b**−**24b** all showed reduced plasma protein binding in rat plasma compared to **2**. The greater free fraction in rat plasma resulted in improved performance in the $FeCl_3$-induced thrombosis assay, even with several compounds (**19a**,**b**, **20a**,**b**, **22b**, **23b**, **24b**) of similar or lesser intrinsic potency than **2**.

Initial screening for pharmacokinetic properties was done in dogs ($n = 2$) using a 1 mg/kg oral dose of amorphous test compound as its trifluoroacetate salt in methocel suspension. Area under the concentration versus time curve (AUC) and plasma half-life data are given in Table 1. In comparing oral AUC values, it is seen that plasma exposures for all of the azafluorenes **17a**,**b**−**20a**,**b** with the exception of **17b** and **19a** were similar to that of the parent compound **2**. Azafluorene-*N*-oxides **21b**−**24b**, however, showed significantly less plasma exposure after oral dosing compared to **2**, and there was a significant drop (10-fold or greater) in AUC for each azafluorene-*N*-oxide compared to its corre-

Table 2. Pharmacokinetic Parameters[a] for Selected Compounds

compd	species	F (%)	CL (mL/min/kg)	V_d (L/kg)	$T_{1/2}$ (h)
20b	dog	88	2.5	1.2	5.5
	monkey	35	1.9	1.2	7.7
	rat	15	53 ± 5	4.5 ± 0.2	1.8 ± 0.2
24b	dog	9	1.0	0.52	5.7
	monkey	5	6.4	2.0	6.3
	rat	1	9.4 ± 2	2.9 ± 1	7.0 ± 0.06
19b	dog	55	0.39	0.43	14
	monkey	57	4.1	2.2	8.2
	rat	22	56 ± 9.5	5.8 ± 3	2.7 ± 0.8

[a] male beagle dogs ($n = 2$) were dosed 1 mg/kg iv and po, male rhesus macaques ($n = 2$) were dosed 1 mg/kg iv and 2 mg/kg po, male Sprague−Dawley rats ($n = 3$) were dosed 2 mg/kg iv and 10 mg/kg po.

sponding azafluorene analogue. The azafluorene-*N*-oxides were found to be significantly more polar than the azafluorenes as determined by log P measurements (values of −1.2 to −0.50 for the azafluorene-*N*-oxides vs 0.2 to 0.5 for the azafluorenes), and so we speculate that the lower plasma exposure of the former may be the result of poor absorption in the gut due to their highly polar nature. Contrary to this argument, however, the plasma exposures of 4-aza-7-chlorofluorenes **25a**,**b** were modest despite their polarities being similar to that of fluorene **2** (log *P* values of 1.1, 1.3, and 1.5, respectively). Plasma half-lives for azafluorenes **17a**,**b**−**20a**,**b** and **25a**,**b** fell into three ranges, short (2−4 h, **17b**, **18a**, **19a**, **25a**, **25b**), intermediate (5−6 h, **17a**, **20a**, **20b**), and long (10−14 h, **18b** and **19b**). For two of the *N*-oxides, **21b** and **24b**, the plasma half-lives were very similar to their corresponding azafluorenyl analogues, and for the other two *N*-oxides, **22b** and **23b**, there was a significant reduction in half-life compared to their corresponding azafluorenyl analogues. The pharmacokinetic behavior of azafluorene **20b** and its *N*-oxide derivative **24b** was examined in greater detail (see Table 2). In three species, the *N*-oxide showed significantly reduced (ca. 10-fold) oral bioavailability compared to the unoxidized azafluorene. In dogs and monkeys, the oral bioavailability and half-life of **20b** were very good. In rats, however, **20b** showed high clearance with a value approaching that of hepatic blood flow, and poor oral bioavailability. In vitro metabolism studies with **20b** using human liver microsomes showed efficient conversion to its *N*-oxide derivative, **24b**. The good oral bioavailability and half-life of **20b** in two species and the good half-life of its *N*-oxide metabolite **24b** in three species lead one to speculate that **20b** dosed in humans might exhibit a pharmacodynamic half-life longer than its pharmacokinetic half-life due to the formation of **24b** as a low clearance active metabolite.

Gratifyingly, the two azafluorenes which exhibited long plasma half-lives in dogs, **18b** and **19b**, were also among the most potent thrombin inhibitors in this series of compounds, and both were fully efficacious for inhibiting $FeCl_3$-induced thrombosis in rats. These two compounds, however, were distinguishable from one another in terms of their stability in human liver microsomes, with **18b** being degraded rapidly and **19b** having good stability. Since this result suggests the potential for a longer half-life for **19b** compared to **18b** in humans, we decided to pursue **19b** further and obtain a more complete set of pharmacokinetic data (see Table 2). As was seen with azafluorene **20b**, clearance of **19b** in the rat was high, and oral bioavailability was on the low side. But in dogs and rhesus monkeys, the oral bioavailability and plasma half-life of **19b** were very favorable. In addition, inhibition of other human serine proteases by **19b** was minimal (K_i trypsin = 2.5 μM; factor Xa = 8.1 μM; chymotrypsin, kallikrein, plasmin, TPA, urokinase >100 μM). Taking into consideration all of our key assays (2xAPTT potency, $FeCl_3$-induced thrombosis assay in rats, oral bioavailability and plasma half-life in three animal species, stability in human liver microsomes, human plasma protein binding), **19b** emerged as the best compound in this series of azafluorenyl P3 inhibitors.

Summary and Conclusion

Modification of a promising series of previously described P2 proline-based thrombin inhibitors by incorporation of a recently discovered P1 group brought about significant improvements in potency and pharmacokinetic properties. The prototype in this new series, **2**, however, was found to lack full efficacy for inhibiting clot formation in an in vivo thrombosis model in rats. Introduction of nitrogen into the tricyclic fluorenyl P3 group of **2** to produce an azafluorenyl ring system proved to be an effective solution to reducing plasma protein binding and restoring full efficacy in the rat thrombosis model. A systematic study of inhibitors containing all possible azafluorene positional isomers, their diastereomers, and *N*-oxides was undertaken. An optimal compound was identified, **19b**, which contains a 3-aza-9-hydroxyfluoren-9(*R*)-yl P3 group. Determination of the stereochemistry of the azafluorenyl P3 group in **19b** was accomplished by X-ray crystallographic analysis of the corresponding azafluorenyl-*N*-oxide derivative **23b** bound in the active site of human thrombin. Compound **19b** was found to be a highly potent inhibitor of thrombin in an isolated enzyme assay (K_i = 0.4 nM) with greater than 5000-fold selectivity for human thrombin vs a panel of other serine proteases. In functional assays, **19b** doubled the activated partial thromboplastin time in human plasma at a concentration of 0.18 μM and fully inhibited $FeCl_3$-induced vessel occlusion in rats with an intravenous infusion of 10 μg/kg/min. Compound **19b** showed excellent pharmacokinetic properties in dogs (F = 55%, iv $T_{1/2}$ = 14 h) and rhesus monkeys (F = 57%, iv $T_{1/2}$ = 8.2 h) and more modest pharmacokinetic properties in rats (F = 22%, iv $T_{1/2}$ = 2.7 h). Compound **19b** also exhibited good stability in the presence of human liver microsomal preparations and maintained a significant free fraction in human plasma protein binding experiments. Taking into consideration all of these key preclinical properties, **19b** represents the best compound to have emerged from our thrombin inhibitor discovery effort to date, and as such offers considerable potential for development as an oral antithrombotic agent.

Experimental Section

All reactions were carried out using commercial grade reagents and solvents. Analytical HPLC data was obtained using an Agilent Zorbax SB−C8 4.6 mm ID × 75 mm 3.5 μm column with a 4.5 min linear gradient from 95:5 to 0:100 A:B (A = 0.1% TFA in water, B = 0.1% TFA in acetonitrile), flow rate = 3 mL/min, UV detection at 215 nm. Reverse phase

preparative HPLC was performed on a Waters Prep LC 4000 using three Waters C_{18} PrepPak 40 × 100 mm columns connected in series, mobile phase was 0.1% TFA in water and 0.1% TFA in acetonitrile with gradients chosen based on the degree of separation and polarity, flow rate = 60 mL/min, UV detection at 215 nm. LC-MS data was obtained on a Waters 2690 analytical HPLC (4 min linear gradient of 92:8 to 0:100 A:B where A = 0.05% TFA in water and B = acetonitrile), flow rate = 1.5 mL/min with detection using a Micromass ZMD mass spectrometer (positive ion electrospray ionization). The ^{1}H NMR spectra were recorded on a Varian Unity Inova 400 MHz spectrometer at 400 MHz with chemical shifts (δ) reported in ppm downfield relative to tetramethylsilane internal standard. High-resolution mass spectroscopy was performed on a Bruker Bio-APEX-11 FTICR/MS with an electrospray ionization mode. The solvent system consisted of acetonitrile/water (50:50% v/v) with 0.1% formic or acetic acid delivered by either direct infusion or auto injection using an HP-1100 sample delivery system. Chemical abbreviations: DIEA = *N*,*N*-diisopropylethylamine; EDC = 1-[3-(dimethylamino)propyl]-3-ethylcarbodiimide hydrochloride; HOBT = 1-hydroxy-benzotriazole hydrate; HOAT = 1-hydroxy-7-azabenzotriazole; MCPBA = meta-chloroperoxybenzoic acid.

L-Prolyl-2-(*tert*-butyloxycarbonylaminomethyl)-5-chlorobenzylamide (7). Step 1. To a stirred solution of **6**[7] (3.80 g, 14.1 mmol, HPLC t_R = 2.63 min), Fmoc-L-Proline (4.98 g, 14.8 mmol, HPLC t_R = 3.26 min), and HOBT (2.15 g, 14.1 mmol) in DMF (30 mL) was added EDC (3.51 g, 18.3 mmol). The pH of the solution was slowly raised to pH 6 (as measured on wetted E. Merck pH indicator strips) by the gradual addition of DIEA (~2 mL). At 2 h reaction time, HPLC analysis indicated complete consumption of the benzylamine starting material. The solvent was removed on a rotary evaporator and the residue was partitioned between EtOAc (200 mL) and water (100 mL). The organic phase was dried ($MgSO_4$), filtered, and the solvent was removed in vacuo. The residue was stirred in ether (100 mL) for several hours and the solid was collected by filtration, washed with ether, and dried to give *N*-fluorenylmethoxycarbonyl-L-prolyl-2-(*tert*-butyloxycarbonyl-aminomethyl)-5-chlorobenzylamide as a white crystalline solid (7.8 g, 94% yield). TLC R_f = 0.5 (1:1 EtOAc:hexanes); HPLC t_R = 3.87 min; LC-MS *m/z* = 590.

Step 2. To a stirred solution of the product from the previous step (7.0 g, 12 mmol) in DMF (50 mL) was added piperidine (7.5 mL). At 15 min reaction time, HPLC analysis indicated complete consumption of the Fmoc-Proline derivative with formation of two new closely eluting components (HPLC t_R = 2.76 min desired product, 2.80 min Fmoc derived byproduct). The solvent and excess piperidine were removed on a rotary evaporator (bath temp 40°C, ~0.5 Torr). The residue was purified on a silica gel column using a gradient elution of 4%, 8%, 12% A in CH_2Cl_2 (A = 95:5 MeOH:NH_4OH) to give **7** as a gum (3.9 g, 90% yield). TLC R_f = 0.4 (90:10:0.5 CH_2Cl_2:MeOH:NH_4OH; iodine visualization); HPLC t_R = 2.77 min; LC-MS *m/z* = 368; ^{1}H NMR, $CDCl_3$, δ 8.04 (br s, 1H), 7.2−7.3 (m, 3H), 5.24 (br s, 1H), 4.4−4.5 (ABX, 2H), 4.28 (d, 2H), 3.80 (dd, *J* = 5.4, 9.4 Hz, 1H), 2.9−3.0 (ABXY, 2H), 2.1−2.2 (m, 1H), 1.9−2.0 (m, 1H), 1.7−1.8 (m, 2H), 1.44 (s, 3H).

9-Hydroxy-9-fluorenylcarbonyl-L-prolyl-2-aminomethyl-5-chlorobenzylamide (2). Step 1. To a stirred solution of **7** (1.0 g, 2.7 mmol), 9-hydroxyfluoren-9-yl carboxylic acid (0.66 g, 2.9 mmol), and HOBT (0.44 g, 2.9 mmol) in DMF (60 mL) was added EDC (0.67 g, 3.5 mmol). DIEA (~0.5 mL) was added dropwise until an aliquot of the reaction spotted on wetted E. Merck pH indicator strips produced a reading of pH 6. The mixture was stirred at ambient temperature for 24 h and then concentrated in vacuo. The residue was partitioned between EtOAc (100 mL) and saturated aqueous $NaHCO_3$ solution (75 mL). The organic phase was dried ($MgSO_4$) and filtered, and the solvent was removed in vacuo. The residue was purified on a silica gel column using 1:1 EtOAc:hexanes as eluant. Product-containing fractions were combined, and the solvent was removed in vacuo to give 9-hydroxy-9-fluorenylcarbonyl-L-prolyl-2-(*tert*-butyloxycarbonylaminomethyl)-5-chlorobenzylamide as a gum (1.4 g, 90% yield). HPLC t_R = 3.69 min; LC-MS *m/z* = 576.

Step 2. A stirred solution of the product from the previous step (1.3 g, 2.2 mmol) in EtOAc (100 mL) was cooled to 0 °C. HCl gas was bubbled through the solution for 15 min, and the mixture was stirred at 0 °C for 1 h. Nitrogen was bubbled through the solution for 15 min to purge excess HCl, and the solvent was removed in vacuo. The resulting solid was suspended in ether (75 mL) and stirred vigorously for 1 h. The solid was collected by filtration to give the HCl salt of **2** (1.0 g, 89% yield). HPLC t_R = 2.83 min; LC-MS *m/z* = 476; ^{1}H NMR, DMSO-d_6: δ 8.69 (br t, 1H), 8.42 (s, 3H), 7.83 (dd, *J* = 7, 2 Hz, 2H), 7.2−7.5 (m, 9H), 6.10 (s, 1H), 4.42 (t, *J* = 5 Hz, 1H), 4.40 (ABX, *J* = 15, 5 Hz, 2H), 4.10 (s, 2H), 2.41 (m, 2H), 1.90 (m, 1H), 1.54 (m, 2H), 1.40 (m, 1H); HRMS (ES/FTMS) $C_{27}H_{26}ClN_3O_3$ calcd 476.1735 (M + 1), found: 476.1738.

4-Aza-9-hydroxy-9-fluorenylcarbonyl-L-prolyl-2-aminomethyl-5-chlorobenzylamide (20a,b). Step 1. To a solution of 2-chloro-3-cyanopyridine (4.06 g, 29.3 mmol) in toluene (60 mL) were added phenylboronic acid (5.4 g, 43.9 mmol), potassium carbonate (6.1 g, 44.1 mmol) and tetrakis(triphenylphosphine)palladium (1.7 g, 1.5 mmol). The mixture was refluxed under nitrogen for 24 h, and the solvent was removed in vacuo. The residue was purified on a silica gel column using 100% CH_2Cl_2 then 99:1 CH_2Cl_2:MeOH as the mobile phase. 2-Phenyl-3-cyanopyridine was obtained as a solid (5.0 g, 94% yield). HPLC t_R = 2.98 min; LC-MS *m/z* = 181; HRMS (ES/FTMS) $C_{12}H_8N_2$ calcd 181.0760 (M + 1), found: 181.0763.

Step 2. The product from the previous step (5.0 g, 27.9 mmol) was dissolved in concentrated hydrochloric acid (140 mL) and heated to reflux for 6 days. The solvent was evaporated in vacuo to yield 2-phenylpyridine-3-carboxylic acid **8** as a solid (7.97 g, 100% yield). HPLC t_R = 1.08 min; LC-MS *m/z* = 200). ^{1}H NMR, 400 MHz (CD_3OD): δ 9.03 (d, *J* = 7.97 Hz, 1H), 8.97−8.95 (m, 1H), 8.18−8.14 (m, 1H), 7.68−7.62 (m, 5H); HRMS (ES/FTMS) $C_{12}H_9NO_2$ calcd 200.0706 (M + 1), found: 200.0683.

Step 3. Acid **8** (7.97 g, 40.0 mmol) and polyphosphoric acid (162 g) were combined and the mixture was heated slowly to 200 °C with mechanical stirring until the acid was fully consumed (7 h). The mixture was cooled to 140 °C, poured carefully over crushed ice, and stirred for 5 h. The solution was extracted several times with CH_2Cl_2. The combined extracts were washed with aqueous sodium bicarbonate, dried over Na_2SO_4, and filtered, and the solvent was removed in vacuo to yield 4-aza-9-fluorenone **9** as a yellow solid (4.7 g, 92% yield over two steps). HPLC t_R = 2.91 min; LC-MS *m/z* = 182; ^{1}H NMR, $CDCl_3$: δ 8.62 (dd, *J* = 5.1, 1.6 Hz, 1H), 7.90 (dd, 7.3, 1.6 Hz, 1H), 7.86 (d, *J* = 7.5 Hz, 1H), 7.74 (d, *J* = 7.5 Hz, 1H), 7.61 (dt, *J* = 1.1, 7.4 Hz, 1H), 7.44 (t, *J* = 7.5 Hz, 1H), 7.22 (dd, *J* = 7.3, 2.1 Hz, 1H); HRMS (ES/FTMS) $C_{12}H_7NO$ calcd 182.0601 (M + 1), found: 182.0588.

Step 4. To a stirred solution of **9** (4.7 g, 25.9 mmol) in CH_2Cl_2 (75 mL) was added zinc iodide (0.81 g, 2.5 mmol) and trimethylsilylcyanide (31 mL, 233 mmol). The mixture was stirred at ambient temperature for 2 h and then heated to reflux for 24 h. The mixture was then blown dry with a stream of nitrogen gas to yield crude 4-aza-9-trimethylsiloxy-9-cyanofluorene (HPLC t_R = 3.71 min; LC-MS *m/z* = 281). This material was dissolved in MeOH (40 mL) and cooled to 0 °C with stirring. The solution was saturated with HCl gas and stirred for 4 h with warming to ambient temperature. The solvent was removed in vacuo, and the residue was partitioned between CH_2Cl_2 and aqueous sodium bicarbonate solution. The CH_2Cl_2 layer was evaporated in vacuo, and the residue was purified on silica gel using 95:5 CH_2Cl_2:MeOH as the mobile phase. 4-Aza-9-hydroxy-9-fluorene carboxylic acid methyl ester **13** was obtained as a solid (4.4 g, 70% yield). ^{1}H NMR, $CDCl_3$: δ 8.58 (dd, *J* = 5.0, 1.2 Hz, 1H), 7.97 (d, *J* = 8.3 Hz, 1H), 7.72 (dd, *J* = 7.5, 1.5 Hz, 1H), 7.50 (dt, *J* = 7.6, 1.6 Hz, 2H), 7.43 (dt, *J* = 7.6, 1.4 Hz, 2H), 7.18 (dd, *J* = 7.6, 5.1 Hz, 1H), 4.45 (s, 1H), 3.63 (s, 3H); HPLC t_R = 2.08 min; LC-MS *m/z* = 242; HRMS (ES/FTMS) $C_{14}H_{11}NO_3$ calcd 242.0812 (M + 1), found: 242.0790.

Step 5. Hydroxy ester **13** (1.9 g, 7.9 mmol) was stirred in hydrazine (10 mL) and the mixture was warmed to 50 °C for 30 min. The reaction mixture was cooled to ambient temperature, and the excess hydrazine was removed in vacuo. The residue was suspended in ether (50 mL) and vigorously stirred for 30 min. The solid was collected by filtration and dried in vacuo to give hydrazide **14** (1.5 g, 85% yield). ^{1}H NMR, DMSO-d_6: δ 9.51 (br s, 1H), 8.52 (dd, J = 5.0, 1.3 Hz, 1H), 7.81 (d, J = 7.0 Hz, 1H), 7.77 (dd, J = 7.5, 1.3 Hz, 1H), 7.4−7.5 (m, 3H), 7.27 (dd, J = 7.5, 5.0 Hz, 1H), 6.70 (s, 1H), 4.30 (br s, 2H); LC-MS m/z = 242; HRMS (ES/FTMS) $C_{13}H_{11}N_3O_2$ calcd 242.0924 (M + 1), found: 242.0928.

Step 6. Hydrazide **14** (1.67 g, 6.9 mmol) was dissolved in DMF (10 mL) and cooled to −20 °C. THF saturated with HCl gas was then added until a drop of the reaction mixture applied to wetted E. Merck pH indicator strip produced a reading of pH 1−2. Amyl nitrite (0.9 mL, 6.9 mmol) was added, and the reaction was stirred at −20 °C until all of the hydrazide was converted to the acyl azide as determined by HPLC and LC-MS analysis (6 h). DIEA was then added until a drop of the reaction mixture applied to wetted E. Merck pH indicator strip produced a reading of pH 6.5. Proline derivative **7** (2.54 g, 6.9 mmol) was then added, and more DIEA was added until a drop of the reaction mixture applied to wetted E. Merck pH indicator strip produced a reading of pH 8. The reaction mixture was stirred at −20 °C until the acyl azide had been completely consumed as determined by HPLC and LC-MS analysis (24 h). The mixture was warmed to ambient temperature and the solvent was removed in vacuo. The residue was purified on a silica gel column using 90:10 CH_2Cl_2:MeOH as the mobile phase. Pure fractions were combined and the solvent was removed in vacuo to give 4-aza-9-hydroxy-9-fluorenylcarbonyl-L-prolyl-2-(*tert*-butyloxycarbonylaminomethyl)-5-chlorobenzylamide **16** as a solid (3.4 g, 85% yield). HPLC t_R = 3.1 min; LC-MS m/z = 577.

Step 7. To a stirred solution of **16** (3.4 g, 5.9 mmol) in CH_2Cl_2 (6 mL) was added TFA (2 mL). The mixture was stirred at ambient temperature for 2 h, and then the solvents were evaporated in vacuo. The residue was purified by preparative reverse phase HPLC using a TFA buffered water:acetonitrile gradient. The resulting mixture of diastereomers was then separated on a Chiralpak AD column (5 × 50 cm, mobile phase of 35% A (A = 0.1% diethylamine in hexane) and 65% EtOH, 60 mL/min flow rate). Using an analytical Chiralpak AD column, 250 × 4.6 mm, 1.5 mL/min flow rate, the two diastereomers had retention times of 5.7 min (**20a**) and 7.9 min (**20b**). The individual diastereomers were run through a preparative reverse phase HPLC using a TFA buffered water:acetonitrile gradient to give, after lyophilization, solid TFA salts of 4-aza-9-hydroxy-9-fluorenylcarbonyl-L-prolyl-2-aminomethyl-5-chlorobenzylamide. **20a** (0.56 g, 20% yield) HPLC t_R = 2.35 min; >99% purity, LC-MS m/z = 477; ^{1}H NMR, $CDCl_3$: δ 8.63 (d, J = 5.04 Hz, 1H), 8.52 (s, 2H), 8.41 (d, J = 5.12 Hz, 1H), 8.02 (d, J = 6.51 Hz, 1H), 7.70 (d, J = 7.78 Hz, 1H), 7.54−7.51 (m, 2H), 7.39 (d, J = 7.33 Hz, 1H), 7.35 (s, 1H), 7.33−7.27 (s,1H), 7.22 (m, 1H),4.91−4.85 (m,1H), 4.45−4.42 (m, 1H), 4.19−4.09 (m,1H), 4.03−3.99 (d, J = 14.74 Hz, 1H), 2.44−2.36 (m, 2H), 1.97−1.88 (m, 1H), 1.80−1.70 (m, 1H), 1.68−1.63 (m, 1H), 1.53−1.45 (m,1H); HRMS (ES/FTMS) $C_{26}H_{25}ClN_4O_3$ calcd 477.1688 (M + 1), found: 477.1681. **20b** (0.45 g, 16% yield) HPLC t_R = 2.35 min; >99% purity, LC-MS m/z = 477; ^{1}H NMR, $CDCl_3$: δ 8.66−8.65 (d, J = 5.31 Hz, 1H), 8.52−8.51 (s, 2H), 8.10 (d, J = 7.60 Hz, 1H), 7.76 (d, J = 7.60 Hz, 1H), 7.57−7.54 (m,1H), 7.47−7.40 (m,2H), 7.37−7.26 (m, 4H), 4.88−4.83 (m, 1H), 4.47−4.44 (m,1H), 4.23−4.00 (m, 2H), 2.32−2.17 (m, 2H), 2.01−1.92 (m,1H), 1.76−1.63 (m, 2H), 1.61−1.45 (m, 1H); HRMS (ES/FTMS) $C_{26}H_{25}ClN_4O_3$ calcd 477.1688 (M + 1), found: 477.1686.

Alternate Synthesis of 4-Aza-9-fluorenone (9). To a three-neck 500 mL round-bottom flask equipped with condenser and addition funnel were added 7,8-benzoquinoline (1.02 g, 5.7 mmol), water (75 mL), and potassium hydroxide (1.1 g, 20.2 mmol). The mixture was heated to reflux, and a hot solution of potassium permanganate (2.6 g, 16.5 mmol) in water (40 mL) was added over 3 h. The hot mixture was filtered. The filtrate was cooled to ambient temperature, extracted with CH_2Cl_2, and dried over $MgSO_4$, and the solvent was removed in vacuo to give **9** (0.2 g, 20% yield).

1-Aza-9-hydroxy-9-fluorenylcarbonyl-L-prolyl-2-aminomethyl-5-chlorobenzylamide (17a,b). Step 1. A solution of 1,4-bis(diphenylphosphino)butane (0.75 g, 1.8 mmol) and bis(benzonitrile)dichloropalladium (0.67 g, 1.8 mmol) in CH_2Cl_2 (30 mL) was stirred at ambient temperature for 20 min, and then the solvent was removed in vacuo. To the residue were added methyl 3-bromopyridine-2-carboxylate[14] (7.4 g, 34.4 mmol), phenylboronic acid (5.5 g, 45.3 mmol), sodium carbonate (7.4 g, 69.8 mmol), and toluene (150 mL). The mixture was heated to reflux for 18 h. The mixture was cooled to ambient temperature, the solids were removed by filtration, and the filtrate solvent was removed in vacuo. The residue was purified on silica gel using 1:2 EtOAc:hexanes as the mobile phase. Pure fractions were combined, and the solvents were removed in vacuo to yield methyl 2-phenyl-1-pyridinecarboxylic acid (5.3 g, 72% yield). HPLC t_R = 2.9 min; LC-MS m/z = 214.

Step 2. To the product from the previous step (5.3 g, 24.9 mmol) dissolved in methanol (100 mL) was added NaOH (1.2 g, 29.9 mmol), and the mixture was stirred at ambient temperature for 1 h. The mixture was neutralized with 1 N HCl (30 mL), and the solvents were removed in vacuo to yield 2-phenylpyridine-1-carboxylic acid (>4.9 g, contains NaCl, 100% yield). HPLC t_R = 1.85 min; LC-MS m/z = 200; HRMS (ES/FTMS) $C_{12}H_9NO_2$ calcd 200.0706 (M + 1), found: 200.0718.

Step 3. The product from the previous step (4.9 g theoretical, 24.6 mmol) was converted to 1-aza-9-fluorenone using the procedure given in Step 3 for **20a**,**b** (4.2 g, 94% yield). HPLC t_R = 2.83 min; LC-MS m/z = 182; ^{1}H NMR, CD_3OD: δ 8.50 (d, J = 6.14 Hz, 1H), 8.13 (d, J = 8.88 Hz, 1H), 7.74 (d, J = 7.42 Hz, 1H), 7.64 (d, J = 7.51 Hz, 1H), 7.62 (m, 1H), 7.52−7.49 (m, 1H), 7.44 (m, 1H); HRMS (ES/FTMS) $C_{12}H_7NO$ calcd 182.0601 (M + 1), found: 182.0592.

Step 4. The product from the previous step (4.2 g, 23.2 mmol) was converted to 1-aza-9-hydroxy-9-fluorene carboxylic acid methyl ester using the procedure given in Step 4 for **20a**,**b** except that acetonitrile was used in place of CH_2Cl_2 as the solvent in the reaction with trimethylsilylcyanide. The product was purified on a silica gel column using 98:2 CH_2Cl_2:MeOH as the mobile phase (4.6 g, 82% yield). HPLC t_R = 2.44 min; LC-MS m/z = 242; ^{1}H NMR, $CDCl_3$: δ 8.48 (d, J = 6.23 Hz, 1H), 7.93 (d, J = 9.16 Hz, 1H), 7.69 (d, J = 7.51 Hz, 1H), 7.55−7.51 (d, J = 7.33 Hz, 1H), 7.47 (m, 1 H), 7.45−7.40 (m, 1H), 7.39−7.30 (m,1H), 3.64 (s, 3H).

Step 5. The product from the previous step (4.6 g, 18.9 mmol) was dissolved in hydrazine (20 mL) and the mixture was stirred at ambient temperature for 2 h. The mixture was evaporated in vacuo and the residue was suspended in CH_2Cl_2. The solid was collected by filtration, washed with CH_2Cl_2, and dried in vacuo to give 1-aza-9-hydroxy-9-fluorene carboxylic acid hydrazide (4.4 g, 96% yield). HPLC t_R = 1.71 min; LC-MS m/z = 242; ^{1}H NMR, CD_3OD: δ 8.37 (d, J = 6.41 Hz, 1H), 8.13 (d, J = 9.16 Hz, 1H), 7.79 (d, J = 7.50 Hz, 1H), 7.53 (d, J = 7.41 Hz, 1H), 7.47−7.36 (m, 3H); HRMS (ES/FTMS) $C_{13}H_{11}N_3O_2$ calcd 242.0924 (M + 1), found: 242.0891.

Step 6. The compound from the previous step (1.2 g, 5 mmol) was converted to 1-aza-9-hydroxy-9-fluorenylcarbonyl-L-prolyl-2-(*tert*-butyloxycarbonylaminomethyl)-5-chlorobenzylamide using the procedure given in Step 6 for **20a**,**b** (1.8 g, 62% yield). HPLC t_R = 3.29 min; LC-MS m/z = 577.

Step 7. The product from the previous step (1.8 g, 3.1 mmol) was deprotected using the same procedure as given in Step 7 for **20a**,**b**. The diastereomers were separated by preparative reverse phase HPLC using a TFA buffered water:acetonitrile gradient. Lyophilization gave solid TFA salts of 1-aza-9-hydroxy-9-fluorenylcarbonyl-L-prolyl-2-aminomethyl-5-chlorobenzylamide. First-eluting diastereomer **17a** (0.5 g, 32% yield) HPLC t_R = 2.53 min; >99% purity, LC-MS m/z = 477; ^{1}H NMR, $CDCl_3$: δ 8.64 (d, J = 4.67 Hz, 1H), 8.3 (s, 2H), 8.07−8.11 (m, 2H), 7.69 (m, 1H), 7.51−7.45 (m, 2H), 7.43−7.41 (m,

1H), 7.32 (s, 1H), 7.22 (d, J = 8.15 Hz, 1H), 7.12 (d, J = 10.07 Hz, 1H), 4.8 (m, 1H), 4.44 (m, 1H), 4.15 (s, 1H), 4.05 (d, J = 12.64 Hz, 1H), 2.64 (m, 2H), 2.04−1.98 (m,1H), 1.75−1.71 (m, 2H), 1.56−1.53 (m, 1H); HRMS (ES/FTMS) $C_{26}H_{25}ClN_4O_3$ calcd 477.1688 (M + 1), found: 477.1683. Second-eluting diastereomer **17b** (0.25 g, 17% yield) HPLC t_R = 2.62 min; >99% purity, LC-MS m/z = 477; ^{1}H NMR, $CDCl_3$: δ 8.49−8.41 (m, 3H), 8.27 (s, 1H), 8.07 (d, J = 8.97 Hz, 1H), 7.71 (d, J = 8.24 Hz, 1H), 7.52−7.42 (m, 4H), 7.35 (s, 1H), 7.32 (s, 1H), 4.68−4.62 (m, 1H), 4.53−4.50 (m, 1H), 4.15−4.11 (m, 2H), 2.55 (s, 1H), 2.43 (m, 1H), 2.05−1.95 (m, 1H), 1.84−1.77 (m, 1H), 1.72−1.65 (m, 1H), 1.57−1.50 (m, 1H); HRMS (ES/FTMS) $C_{26}H_{25}ClN_4O_3$ calcd 477.1688 (M + 1), found: 477.1683.

2-Aza-9-hydroxy-9-fluorenylcarbonyl-L-prolyl-2-aminomethyl-5-chlorobenzylamide (18a,b). Step 1. 4-Phenylpyridine-3-carboxylic acid methyl ester[13] (3.8 g, 17.8 mmol) was hydrolyzed to 4-phenylpyridine-3-carboxylic acid using the procedure given in Step 2 for **17a**,**b** (4.7 g, theoretical yield = 3.6 g, balance is NaCl). HPLC t_R = 1.80 min; LC-MS m/z = 200; ^{1}H NMR, CD_3OD: δ 8.91 (s, 1H), 8.66 (d, J = 5.22 Hz, 1H), 7.48 (d, J = 5.22 Hz, 1H), 7.46−7.41 (m, 5H).

Step 2. The compound from the previous step (4.7 g, 23.8 mmol) was converted to 2-aza-9-fluorenone using the procedure given in Step 3 for **20a**,**b** except that extraction of the product into CH_2Cl_2 required prior neutralization of the polyphosphoric acid with 50% aqueous NaOH to pH 4 (3.1 g, 71% yield). HPLC t_R = 2.16 min; LC-MS m/z = 182); ^{1}H NMR, $CDCl_3$: δ 8.87 (s, 1H), 8.75 (d, J = 4.95 Hz, 1H), 7.75 (d, J = 7.33 Hz, 1H), 7.65 (d, J = 7.50 Hz, 1H), 7.62−7.55 (m, 1H), 7.51−7.46 (m, 2H); HRMS (ES/FTMS) $C_{12}H_7NO$ calcd 182.0601 (M + 1), found: 182.0613.

Step 3. The compound from the previous step (3.1 g, 17.2 mmol) was converted to 2-aza-9-hydroxy-9-fluorene carboxylic acid methyl ester using the procedure given in Step 4 for **20a**,**b**, except that additional amounts of zinc iodide and trimethylsilyl cyanide and a longer reaction time were required for complete conversion of the ketone to the trimethylsilyl cyanohydrin. The product was purified on a silica gel column using 95:5 CH_2Cl_2:MeOH as the mobile phase (1.3 g, 31% yield). HPLC t_R = 2.06 min; LC-MS m/z = 242); ^{1}H NMR, $CDCl_3$: δ 8.67−8.65 (m, 2H), 7.75 (d, J = 6.96 Hz, 1H), 7.57 (d, J = 5.04 Hz, 1H), 7.51−7.44 (m, 3H), 4.50 (s, 1H), 3.64 (s, 3H); HRMS (ES/FTMS) $C_{14}H_{11}NO_3$ calcd 242.0812 (M + 1), found: 242.0780.

Step 4. The product from the previous step (1.4 g, 5.8 mmol) was converted to 2-aza-9-hydroxy-9-fluorene carboxylic acid hydrazide using the same procedure as given in Step 5 for **17a**,**b** (1.4 g, 99% yield). HPLC t_R = 0.8 min; LC-MS m/z = 242; ^{1}H NMR, CD_3OD: δ 8.58 (s, 1H), 8.55 (d, 1H), 7.9−7.85 (m, 1H), 7.78 (d, 1H), 7.59−7.54 (m, 1H), 7.52−7.47 (m, 2H). HRMS (ES/FTMS) $C_{13}H_{11}N_3O_2$ calcd 242.0924 (M + 1). Found: 242.0916.

Step 5. The product from the previous step (1.4 g, 5.8 mmol) was converted to 2-aza-9-hydroxy-9-fluorenylcarbonyl-L-prolyl-2-(*tert*-butyloxycarbonylaminomethyl)-5-chlorobenzylamide using the procedure given in Step 6 for **20a**,**b** (0.27 g, 8% yield). HPLC t_R = 2.75 min; LC-MS m/z = 577; ^{1}H NMR, $CDCl_3$: δ 8.90−8.66 (m, 2H), 7.98−7.90 (m, 2H), 7.68−7.54 (m, 2H), 7.49 (d, J = 7.15 Hz, 1H), 7.30−7.23 (m, 2H), 7.20 (s, 1H), 5.45 (s, 1H), 4.63−4.54 (m, 2H), 4.31 (s, 2H), 2.46−2.26 (m, 2H), 2.03−1.87 (m, 2H), 1.81−1.71 (m, 1H), 1.58−1.49 (m, 1H), 1.42 (s, 9H); HRMS (ES/FTMS) $C_{31}H_{33}ClN_4O_5$ calcd 577.2212 (M + 1), found: 577.2185.

Step 6. The product from the previous step (0.27 g, 0.47 mmol) was deprotected using the same procedure as given in Step 7 for **20a**,**b**. The crude product was purified by preparative reverse phase HPLC using a TFA buffered water:acetonitrile gradient. The diastereomers were then separated on a Deltapak C18 column (40 × 100 mm, 3 in series) with a mobile phase gradient of 85% A, 15% B to 60% A, 40% B (A = 0.1% NH_4OAc in water, B = acetonitrile) over 1 h, flow rate = 50 mL/min. On an analytical column using a similar mobile phase, the first-eluting diastereomer had a retention time of 3.50 min (**18a**) and the second-eluting diastereomer had a retention time of 4.72 min (**18b**). Each diastereomer was then run through a preparative reverse phase HPLC using a TFA buffered water:acetonitrile gradient to give, after lyophilization, solid TFA salts of 2-aza-9-hydroxy-9-fluorenylcarbonyl-L-prolyl-2-aminomethyl-5-chlorobenzylamide. **18a** (40 mg, 18% yield) HPLC t_R = 2.25 min; >99% purity, LC-MS m/z = 477; ^{1}H NMR, CD_3OD: δ 8.80−8.76 (m, 2H), 8.27 (d, J = 5.68 Hz, 1H), 8.12−8.09 (m, 1H), 7.67−7.63 (m, 2H), 7.62−7.55 (m, 1H), 7.49 (d, J = 2.01 Hz, 1H), 7.44−7.38 (m, 2H), 4.56 (d, J = 15.2 Hz, 1H), 4.46−4.42 (m, 1H), 4.30 (d, J = 15.39 Hz, 1H), 4.26 (s, 2H), 3.19−3.09 (m, 1H), 2.98−2.95 (m, 1H), 2.10 (m, 1H), 1.82−1.68 (m, 3H). HRMS (ES/FTMS) $C_{26}H_{25}ClN_4O_3$ calcd 477.1688 (M + 1), found: 477.1680. **18b** (34 mg, 13% yield) HPLC t_R = 2.28 min; >99% purity, LC-MS m/z = 477); ^{1}H NMR, CD_3OD: δ 8.76 (d, J = 5.5 Hz, 1H), 8.64 (s, 1H), 8.16 (d, J = 5.68 Hz, 1H), 8.08−8.06 (m, 1H), 7.66−7.60 (m, 2H), 7.59−7.57 (m, 1H), 7.50 (d, J = 1.83 Hz, 1H), 7.45−7.39 (m, 2H), 4.60 (d, J = 15.2 Hz, 1H), 4.47−4.44 (m, 1H), 4.30−4.26 (m, 3H), 2.72 (s, 2H), 2.08−2.04 (m, 1H), 1.73−1.65 (m, 2H), 1.64−1.56 (m, 1H). HRMS (ES/FTMS) $C_{26}H_{25}ClN_4O_3$ calcd 477.1688 (M + 1), found: 477.1658.

3-Aza-9-hydroxy-9-fluorenylcarbonyl-L-prolyl-2-aminomethyl-5-chlorobenzylamide (19a,b). Step 1. To a solution of methyl 3-bromopyridine-4-carboxylate[14] (5.9 g) in toluene (140 mL) were added phenylboronic acid (4.3 g, 35.2 mmol), potassium carbonate (4.9 g, 35.3 mmol), and tetrakis-(triphenylphosphine)palladium (1.4 g, 1.18 mmol). The mixture was heated to reflux under nitrogen for 4 h, cooled to ambient temperature, and filtered. The filtrate solvent was removed in vacuo, and the residue was purified on a silica gel column using 1:2 EtOAc:hexanes as the mobile phase. Pure fractions were combined and the solvents were removed in vacuo to yield 3-phenylpyridine-4-carboxylic acid methyl ester (3.6 g, 80% yield). HPLC t_R = 2.70 min; LC-MS m/z = 214; ^{1}H NMR, $CDCl_3$: δ 8.74 (overlapping s and d, 2H); 7.65 (d, J = 8 Hz, 1H); 7.4−7.5 (m, 3 H), 7.30−7.35 (m, 2H); 3.80 (s, 3H).

Step 2. The product from the previous step (3.6 g, 16.7 mmol) was converted to 3-phenylpyridine-4-carboxylic acid using the procedure given in Step 2 for **17a**,**b** (4.5 g, theoretical yield = 3.3 g, balance is NaCl). HPLC t_R = 1.22 min; LC-MS m/z = 200; HRMS (ES/FTMS) $C_{12}H_9NO_2$ calcd 200.0706 (M + 1), found: 200.0695.

Step 3. The product from the previous step (4.5 g, 18.2 mmol theoretical) was converted to 3-aza-9-fluorenone using the procedure given in Step 3 for **20a**,**b** except that extraction of the product into CH_2Cl_2 required prior neutralization of the polyphosphoric acid with 50% aqueous NaOH to pH 4 (2.9 g, 95% yield over two steps). HPLC t_R = 2.41 min; LC-MS m/z = 182; ^{1}H NMR, CD_3OD: δ 8.94 (s, 1H), 8.65 (d, J = 4.76 Hz, 1H), 7.82 (d, J = 7.33 Hz, 1H), 7.71 (d, J = 7.32 Hz, 1H), 7.64−7.62 (m, 1H), 7.56 (d, J = 4.40 Hz, 1H), 7.46−7.42 (m, 1H); HRMS (ES/FTMS) $C_{12}H_7NO$ calcd 182.0601 (M + 1), found: 182.0592.

Step 4. The product from the previous step (2.9 g, 16 mmol) was converted to 3-aza-9-hydroxy-9-fluorene carboxylic acid methyl ester using the procedure given in Step 4 for **20a**,**b** except that neat trimethylsilyl cyanide was used in the conversion of the ketone to the trimethylsilyl cyanohydrin. The product was purified on a silica gel column using 1:1 EtOAc:hexanes as the mobile phase (2.2 g, 57% yield). HPLC t_R = 2.00 min; LC-MS m/z = 242; ^{1}H NMR, $CDCl_3$: δ 8.93 (s, 1H); 8.56 (d, J = 5 Hz, 1H); 7.76 (d, J = 7.5 Hz, 1H); 7.48 (t, J = 7 Hz, 2H); 7.38 (t, J = 7 Hz, 2H); 4.60 (s, 1H), 3.62 (s, 3H); HRMS (ES/FTMS) $C_{14}H_{11}NO_3$ calcd 242.0812 (M + 1), found: 242.0818.

Step 5. The product from the previous step (2.2 g, 9.1 mmol) was converted to 3-aza-9-hydroxy-9-fluorene carboxylic acid hydrazide using the procedure given in Step 5 for **17a**,**b** (2.0 g, 90% yield). HPLC t_R = 0.7 min; LC-MS m/z = 242; ^{1}H NMR, DMSO-d_6: δ 9.51 (br s, 1H); 9.04 (s, 1H); 8.51 (d, J = 4 Hz, 1H); 7.89 (d, J = 7 Hz, 1H); 7.4−7.5 (m, 3H), 7.35 (t, J = 6 Hz, 1H); 6.78 (s, 1H); HRMS (ES/FTMS) $C_{13}H_{11}N_3O_2$ calcd 242.0924 (M + 1), found: 242.0939.

Step 6. The product from the previous step (1.1 g, 4.6 mmol) was converted to 3-aza-9-hydroxy-9-fluorenylcarbonyl-L-prolyl-2-(*tert*-butyloxycarbonylaminomethyl)-5-chlorobenzylamide using the procedure given in Step 6 for **20a**,**b** except that the crude product was first purified on a silica gel column using a gradient mobile phase of 99:1 to 96:4 CH_2Cl_2:MeOH, followed by preparative reverse phase HPLC using a TFA buffered water:acetonitrile gradient (0.34 g, 13% yield). HPLC $t_R = 2.99$ min; LC-MS $m/z = 577$. The mixture of diastereomers so obtained could be used directly in the next step as described below, or they could be separated at this stage on a Chiralcel OD 5 × 50 cm column (mobile phase 80% A, where A = 0.1% diethylamine in hexane, 20% 2-propanol, flow rate = 80 mL/min). On an analytical Chiralcel OD column (250 × 4.6 mm, same mobile phase as above, flow rate = 2.0 mL/min), the first-eluting diastereomer had a retention time of 4.89 min and the second-eluting diastereomer had a retention time of 7.37 min. Upon deprotection with TFA, the first-eluting diastereomer produced **19a** and the second-eluting diastereomer produced **19b**.

Step 7. The product from the previous step (0.34 g, 0.59 mmol) was deprotected using the same procedure as given in Step 7 for **20a**,**b**. Separation of the closely eluting diastereomers required multiple passes on a preparative reverse phase HPLC and a TFA buffered water:acetonitrile gradient (99:1 to 50:50 A:B, where A = 0.1% TFA in H_2O, B = 0.1% TFA in CH_3CN). Lyophilization gave solid TFA salts of 3-aza-9-hydroxy-9-fluorenylcarbonyl-L-prolyl-2-aminomethyl-5-chlorobenzylamide. First-eluting diastereomer **19a** (10 mg, 4% yield) HPLC $t_R = 2.20$ min; >99% purity, LC-MS $m/z = 477$); ^{1}H NMR, CD_3OD: δ 9.15 (s, 1H), 8.65 (d, $J = 5.13$, 1H), 7.98 (d, $J = 7.6$, 1H), 7.74 (d, $J = 5.31$, 1H), 7.60−7.56 (m, 1H), 7.51 (s, 3H), 7.46−7.40 (m, 2H), 4.60−4.56 (d, $J = 15.2$, 1H), 4.44−4.41 (m, 1H), 4.34−4.31 (d, $J = 15.2$, 1H), 4.27 (s, 2H), 2.89−2.82 (m, 2H), 2.09−2.03 (m, 1H), 1.86−1.61 (m, 3H); HRMS (ES/FTMS) $C_{26}H_{25}ClN_4O_3$ calcd 477.1688 (M + 1), found: 477.1685. Second-eluting diastereomer **19b** (6 mg, 2% yield) HPLC $t_R = 2.24$ min; >99% purity, LC-MS $m/z = 477$; ^{1}H NMR, CD_3OD: δ 9.16 (s, 1H), 8.66 (d, $J = 5.22$, 1H), 8.00 (d, $J = 7.51$, 1H), 7.69 (d, $J = 5.12$, 1H), 7.60−7.55 (m, 1H), 7.53−7.47 (m, 3H), 7.45−7.42 (m, 2H), 4.62−4.58 (d, $J = 15.2$, 1H), 4.47−4.37 (m, 1H), 4.32 (s, 1H), 4.28 (s, 2H), 2.70 (s, 2H), 2.29−2.02 (m, 1H), 1.90−1.64 (m, 2H), 1.60−1.56 (m, 1H); HRMS (ES/FTMS) $C_{26}H_{25}ClN_4O_3$ calcd 477.1688 (M + 1), found: 477.1689.

3-Aza-9-hydroxyfluoren-9(*R*)-ylcarbonyl-L-prolyl-2-aminomethyl-5-chlorobenzylamide (19b). An alternate, higher yielding synthesis of **19b** was accomplished as follows.

Step 1. 3-Aza-9-hydroxy-9-fluorene carboxylic acid methyl ester (3.6 g) was prepared as described above. The two enantiomers were separated on a preparative Chiralpak AD column (5 × 50 cm) using an 82:18 mixture of A:EtOH (A = 0.1% TFA in hexanes) as the mobile phase. The second-eluting enantiomer was collected, and the solvents were removed in vacuo. The residue was partitioned between EtOAc and saturated aqueous $NaHCO_3$. The aqueous phase was extracted with EtOAc, and the combined organic extracts were evaporated in vacuo to give 1.0 g of the (−) enantiomer of 3-aza-9-hydroxy-9-fluorene carboxylic acid methyl ester. On an analytical column (250 × 4.6 mm Chiralpak AD column, mobile phase 75:25 A:EtOH, A = 0.1% TFA in hexanes, 1.5 mL/min flow rate), the (−) enantiomer had a retention time of 7.6 min, and the (+) enantiomer had a retention time of 6.3 min.

Step 2. The ester from the previous step (1.0 g, 4.1 mmol) was converted to 3-aza-9-hydroxy-9-fluorene carboxylic acid hydrazide (0.81 g, 81% yield) using the procedure given above for the racemic ester.

Step 3. The product from the previous step (0.73 g, 3.0 mmol) was converted to 3-aza-9-hydroxy-9-fluorenylcarbonyl-L-prolyl-2-(*tert*-butyloxycarbonylaminomethyl)-5-chlorobenzylamide using the procedure given in Step 6 for **20a**,**b** except after the pH was adjusted to 6.5, molecular sieves were added followed by HOAT (0.4 g, 3.1 mmol). The pH was adjusted to 7 with DIEA, and the temperature was maintained at −26 ° C until conversion of the active ester to the amide was complete as determined by HPLC and LC-MS (48 h). The mixture was warmed to ambient temperature, the solvent was removed in vacuo, and the residue was purified by preparative reverse-phase HPLC using a 99:1 to 45:55 A:B mobile phase gradient over 1 h, A = 0.1% TFA in water, B = 0.1% TFA in acetonitrile. (0.9 g, 44% yield).

Step 4. The product from the previous step (0.9 g, 1.6 mmol) was deprotected using the same procedure as given in Step 7 for **20a**,**b**. Purification by preparative reverse-phase HPLC using a gradient of 99:1 to 50:50 A:B (A = 0.1% TFA in water, B = 0.1% TFA in acetonitrile) over 1 h followed by lyophilization gave the TFA salt of **19b** as a solid (0.6 g, 92% yield).

General Procedure for the Preparation of *N*-Oxides 21a,b−24a,b. Each of the azafluorene diastereomers **17a**,**b**−**20a**,**b** was converted to its corresponding azafluorene *N*-oxide derivative as exemplified with the three-step procedure given below for the preparation of **24b**.

4-Aza-9-hydroxy-9-fluorenylcarbonyl-L-prolyl-2-aminomethyl-5-chlorobenzylamide, *N*-Oxide (24b). Step 1. To a stirred solution of **20b** (0.10 g, 0.21 mmol) in DMF (2 mL) were added di-*tert*-butyl-dicarbonate (30 mg, 0.15 mmol) and DIEA (31 μL, 0.17 mmol). The mixture was stirred at ambient temperature for 16 h and then evaporated in vacuo. The residue was partitioned between EtOAc and water. The organic phase was washed with water and dried (Na_2SO_4) to yield 4-aza-9-hydroxy-9-fluorenylcarbonyl-L-prolyl-2-(*tert*-butyloxycarbonylaminomethyl)-5-chlorobenzylamide (0.11 g, 91% yield). HPLC $t_R = 3.1$ min; LC-MS $m/z = 577$.

Step 2. The product from the previous step (0.11 g, 0.19 mmol) was dissolved in CH_2Cl_2 (2 mL) and cooled to 0 °C. MCPBA (50 mg, 0.3 mmol) was added, and the mixture was stirred for 16 h while allowing the cooling bath to warm to ambient temperature. The solvent was evaporated in vacuo, and the residue was purified by preparative reverse phase HPLC using a TFA buffered water:acetonitrile gradient to yield 4-aza-9-hydroxy-9-fluorenylcarbonyl-L-prolyl-2-(*tert*-butyloxycarbonylaminomethyl)-5-chlorobenzylamide, *N*-oxide(50 mg, 44% yield). HPLC $t_R = 3.1$ min; LC-MS $m/z = 593$.

Step 3. To a stirred solution of the product from the previous step (50 mg, 0.087 mmol) in CH_2Cl_2 (4 mL) was added TFA acid (2 mL). The mixture was stirred for 1 h and then evaporated in vacuo. The residue was purified on a preparative reverse phase HPLC using a TFA buffered water:acetonitrile gradient. Lyophilization yielded a solid TFA salt of **24b** (40 mg, 95% yield). HPLC $t_R = 2.30$ min; LC-MS $m/z = 493$; ^{1}H NMR, CD_3OD: δ 8.64−8.60 (m, 1H), 8.37−8.34 (m, 1H), 7.64−7.43 (m, 8H), 4.63−4.57 (m, 1H), 4.46−4.42 (m, 1H), 4.32−4.28 (m, 2H), 3.32 (m, 1H), 2.77−2.73 (m, 2H), 2.10−2.03 (m, 1H), 1.79−1.56 (m,3H); HRMS (ES/FTMS) $C_{26}H_{25}ClN_4O_4$ calcd 493.1637 (M + 1), found: 493.1628.

4-Aza-9-hydroxy-9-fluorenylcarbonyl-L-prolyl-2-aminomethyl-5-chlorobenzylamide, *N*-Oxide (24a). Compound **20a** was the starting material for **24a**. HPLC $t_R = 2.29$ min; LC-MS $m/z = 493$; ^{1}H NMR, CD_3OD: δ 8.60 (d, $J = 8.24$ Hz, 1H), 8.33 (d, $J = 6.41$ Hz, 1H), 7.62−7.55 (m, 3H), 7.51 (s, 2H), 7.45−7.40 (m, 3H), 4.58−4.54 (d, $J = 15.2$ Hz, 1H), 4.43−4.39 (m, 1H), 4.33−4.30 (d, $J = 15.2$ Hz, 1H), 4.26 (s, 2H), 2.99 (s, 1H), 2.86 (s, 1H), 2.07−2.05 (m, 1H), 1.77−1.63 (m, 3H); HRMS (ES/FTMS) $C_{26}H_{25}ClN_4O_4$ calcd 493.1637 (M + 1), found: 493.1629.

1-Aza-9-hydroxy-9-fluorenylcarbonyl-L-prolyl-2-aminomethyl-5-chlorobenzylamide, *N*-Oxide (21a,b). Compound **17a** was the starting material for **21a.** HPLC $t_R = 2.37$ min; LC-MS $m/z = 493$; ^{1}H NMR, CD_3OD: δ 8.02−7.95 (s, 1H), 7.92 (d, $J = 7.33$ Hz, 1H), 7.88 (d, $J = 7.51$ Hz, 1H), 7.56−7.51 (m, 5H), 7.49−7.38 (s, 2H), 4.68−4.28 (m, 3H), 4.25−4.23 (m, 2H), 3.33−3.29 (m, 2H), 2.18−2.05 (s, 1H), 1.90 (s, 3H); HRMS (ES/FTMS) $C_{26}H_{25}ClN_4O_4$ calcd 493.1637 (M + 1), found: 493.1642. Compound **17b** was the starting material for **21b.** HPLC $t_R = 2.53$ min; LC-MS $m/z = 493$; ^{1}H NMR, CD_3OD: δ 8.15 (d, $J = 6.50$ Hz, 1H), 8.01 (d, $J = 7.69$ Hz, 1H), 7.94 (d, $J = 7.60$ Hz, 1H), 7.67−7.62 (m, 1H), 7.60 (s, 2H), 7.58−7.39 (m, 4H), 4.58−4.54 (m, 1H), 4.49−4.38 (m, 2H),

4.33−4.24 (m, 2H), 2.53−2.42 (m, 2H), 2.15−2.05 (m, 1H), 1.83−1.78 (m, 1H), 1.76−1.53 (m, 2H); HRMS (ES/FTMS) $C_{26}H_{25}ClN_4O_4$ calcd 493.1637 (M + 1), found: 493.1640.

2-Aza-9-hydroxy-9-fluorenylcarbonyl-L-prolyl-2-aminomethyl-5-chlorobenzylamide, *N*-Oxide (22a,b). Compound **18a** was the starting material for **22a**. HPLC t_R = 2.35 min; LC-MS *m/z* = 493; ^{1}H NMR, CD_3OD: δ 8.38−8.36 (m, 1H), 8.34 (s, 1H), 7.92−7.88 (m, 2H), 7.61−7.55 (m, 1H), 7.54−7.47 (m, 3H), 7.43−7.36 (m, 2H), 4.61−4.57 (d, J = 15.02 Hz, 1H), 4.44−4.40 (m, 1H), 4.27−4.17 (m, 3H), 3.31−3.23 (m, 1H), 3.21−3.05 (m, 1H), 2.14−2.10 (m, 1H), 1.84−1.79 (m, 1H), 1.76−1.69 (m, 2H); HRMS (ES/FTMS) $C_{26}H_{25}ClN_4O_4$ calcd 493.1637 (M + 1), found: 493.1641. Compound **18b** was the starting material for **22b.** HPLC t_R = 2.41 min; LC-MS *m/z* = 493); ^{1}H NMR, CD_3OD: δ 8.39−8.37 (d, J = 8.14 Hz, 1H), 8.04 (s, 1H), 7.93−7.90 (m, 2H), 7.59−7.54 (m, 2H), 7.52−7.45 (m, 2H), 7.43−7.38 (m, 2H), 4.79−4.74 (m, 1H), 4.57−4.53 (d, J = 15.11 Hz, 1H), 4.50−4.47 (m, 1H), 4.30−4.24 (m, 2H), 2.59−2.50 (m, 2H), 2.03−1.67 (m, 1H), 1.66−1.53 (m, 2H); HRMS (ES/FTMS) $C_{26}H_{25}ClN_4O_4$ calcd 493.1637 (M + 1), found: 493.1642.

3-Aza-9-hydroxy-9-fluorenylcarbonyl-L-prolyl-2-aminomethyl-5-chlorobenzylamide, *N*-Oxide (23a,b). Compound **19a** was the starting material for **23a.** HPLC t_R = 2.31 min; LC-MS *m/z* = 493; HRMS (ES/FTMS) $C_{26}H_{25}ClN_4O_4$ calcd 493.1637 (M + 1), found: 493.1653. Compound **19b** was the starting material for **23b.** HPLC t_R = 2.35 min; LC-MS *m/z* = 493; HRMS (ES/FTMS) $C_{26}H_{25}ClN_4O_4$ calcd 493.1637 (M + 1), found: 493.1638.

1-Aza-7-chloro-9-hydroxy-9-fluorenylcarbonyl-L-prolyl-2-aminomethyl-5-chlorobenzylamide (25a,b). Step 1. 4-Aza-7-chloro-9-fluorenone[15] (4.2 g, 19.6 mmol) was converted to 4-aza-7-chloro-9-hydroxy-9-fluorene carboxylic acid methyl ester using the procedure as given in Step 4 of **20a**,**b** (4.8 g, 89% yield) HPLC t_R = 2.55 min; LC-MS *m/z* = 276.

Step 2. The product from the previous step (4.1 g, 19.2 mmol) was converted to 4-aza-7-chloro-9-hydroxy-9-fluorene-carboxylic acid hydrazide using the procedure of Step 5 of **17a**,**b** (3.8 g, 72% yield). HPLC t_R = 1.75 min; LC-MS *m/z* = 276; HRMS (ES/FTMS) $C_{13}H_{10}ClN_3O_2$ calcd 276.0534 (M + 1), found: 276.0539.

Step 3. The product from the previous step (0.7 g, 2.6 mmol)-was converted to 4-aza-7-chloro-9-hydroxy-9-fluorenylcarbonyl-L-prolyl-2-(*tert*-butyloxycarbonylaminomethyl)-5-chlorobenzylamide using the procedure given in Step 6 of **20a**,**b** (0.42 g, 27%). HPLC t_R = 3.39 min; LC-MS *m/z* = 611.

Step 4. The product from the previous step (0.4 g, 0.7 mmol) was deprotected using the procedure of Step 7 of **20a**,**b**. The crude product was purified by preparative reverse phase HPLC using a TFA buffered water:acetonitrile mobile phase. The diastereomers were then separated by preparative reverse phase HPLC using an ammonium bicarbonate buffered mobile phase (Deltapak C18 column, 40 × 100 mm, 3 columns in series, flow rate = 50 mL/min, gradient of 95% A, 5% B to 5% A, 95% B over 1 h where A = 0.1% NH_4HCO_3 in H_2O and B = acetonitrile). Analysis on an analytical Delta Pak C18 column, 150 × 3.5 mm, flow rate = 1.0 mL/min, using a mobile phase of 70% A (where A = 0.1% NH_4OAc in water) 30% B (where B = CH_3CN) showed the first peak to elute at 7.52 min. (**25a)** and the second at 9.20 min. (**25b)**. The individual diastereomers were then passed though a preparative reverse phase HPLC using a TFA buffered water:acetonitrile mobile phase followed by lyophilization to give solid TFA salts of 4-aza-7-chloro-9-hydroxy-9-fluorenylcarbonyl-L-prolyl-2-aminomethyl-5-chlorobenzylamide. First-eluting diastereomer **25a** (80 mg, 19% yield, HPLC t_R = 2.58 min; >99% purity, LC-MS *m/z* = 511); ^{1}H NMR, CD_3OD: δ 8.58 (d, J = 6.41 Hz, 1H), 7.94 (d, J = 8.24 Hz, 1H), 7.83 (m, 1H), 7.56 (m, 1H), 7.50 (s, 2H), 7.42 (m, 2H), 7.38−7.35 (m, 1H), 4.60 (d, J = 15.01 Hz, 1H), 4.43−4.39 (m, 1H), 4.32 (s, 1H), 4.28 (s, 1H), 4.27 (s, 1H), 2.67−2.63 (m, 2H), 2.08−1.99 (m, 1H), 1.74−1.61 (m,2H), 1.59−1.54 (m, 1H). HRMS (ES/FTMS) $C_{26}H_{24}Cl_2N_4O_3$ calcd 511.1298 (M + 1). Found: 511.1292. Second-eluting diastereomer **25b** (80 mg, 19% yield, HPLC t_R = 2.60 min; >99% purity, LC-MS *m/z* = 511); ^{1}H NMR, CD_3OD: δ 8.59 (d, J = 6.22 Hz, 1H), 7.95 (d, J = 8.06 Hz, 1H), 7.80 (d, J = 8.97 Hz, 1H), 7.60−7.57 (m, 1H), 7.52−7.46 (m, 2H), 7.44−7.41 (m, 2H), 7.39−7.36 (m, 1H), 4.61 (d, J = 15.2 Hz, 1H), 4.44−4.41 (m, 1H), 4.30 (s, 1H), 4.27 (s, 2H), 2.71−2.60 (m,1H), 2.59−2.54 (m,1H), 2.11−2.02 (m,1H), 1.72−1.56 (m,3H). HRMS (ES/FTMS) $C_{26}H_{24}Cl_2N_4O_3$ calcd 511.1298 (M + 1). Found: 511.1293.

Acknowledgment. The authors would like to thank Dr. Harri Ramjit, Dr. Art Coddington, and Dr. Charles Ross for high resolution mass spectroscopy data, Dr. Sandor Varga and Mrs. Joan Murphy for NMR support, Ms. Amada Strzelec, Mr. Ken Anderson and Ms. Kristi Hoffman for log P determinations and Mrs. Bang-Lin Wan for rat PK determinations. We would also like to thank Dr. Stephen Brady, Dr. Terry Lyle, Dr. Jules Shafer, Dr. Joseph Vacca and Dr. Joel Huff for their guidance, encouragement, and support.

References

(1) Hauptmann, J. Pharmacokinetics of an Emerging New Class of Anticoagulant/Antithrombotic Drugs. A Review of Small-Molecule Thrombin Inhibitors. *Eur. J. Clin. Pharm.* **2002**, *57*, 751−758.

(2) Crowther, M. A.; Weitz, J. I. Ximelagatran: the first oral direct thrombin inhibitor. *Expert Opin. Invest. Drugs* **2004**, *13*, 403−413.

(3) Brady, S. F.; Stauffer, K. J.; Lumma, W. C.; Smith, G. M.; Ramjit, H. G.; Lewis, S. D.; Lucas, B. J.; Gardell, S. J.; Lyle, E. A.; Appleby, S. D.; Cook, J. J.; Holahan, M. A.; Stranieri, M. T.; Lynch, J. J.; Lin, J. H.; Chen, I. W.; Vastag, K.; Naylor-Olsen, A. M.; Vacca, J. P. Discovery and Development of L-372, 460, a Novel Potent Orally Active Small Molecule Inhibitor of Thrombin: Co-application of Structure-Based Design and Rapid Multiple Analogue Synthesis on Solid Support. *J. Med. Chem.* **1998**, *41*, 401−406.

(4) Lumma, W. C.; Witherup, K. M.; Tucker, T. J.; Brady, S. F.; Sisko, J. T.; Naylor-Olsen, A. M.; Lewis, S. D.; Freidinger, R. M. Design of Novel, Potent, Noncovalent Inhibitors of Thrombin with Nonbasic P1 Substructures. Rapid Structure−Activity Studies by Solid-Phase Synthesis. *J. Med. Chem.* **1998**, *41*, 3687−3693.

(5) Rittle, K. E.; Barrow, J. C.; Nantermet, P. G.; Newton, C. L.; Krueger, J. A.; Lewis, S. D.; Lucas, B. J.; Selnick, H. G. Unexpected Enhancement of Potency With ortho-Aminoalkylbenzylamides in the P1 Position. *Bioorg. Med. Chem. Lett.* **2003** *13*, 3477−3482.

(6) Tucker, T. J.; Lumma, W. C.; Lewis, S. D.; Gardell, S. J.; Lucas, B. J.; Baskin, E. P.; Woltmann, R.; Lynch, J. J.; Lyle, E. A.; Appleby, S. D.; Chen, I. W.; Dancheck, K. B.; Vacca, J. P. Potent Noncovalent Thrombin Inhibitors that Utilize the Unique Amino Acid D-Dicyclohexylalanine in the P3 Position. Implications on Oral Bioavailability and Antithrombotic Activity. *J. Med. Chem.* **1997**, *40*, 1565−1569.

(7) Nelson, T. D.; LeBlond, C. R.; Frantz, D. E.; Matty, L.; Mitten, J. V.; Weaver, D. G.; Moore, J. C.; Kim, J.; Boyd, R.; Kim, P.-Y.; Gbewonyo, K.; Brower, M.; Sturr, M.; McLaughlin, K.; McMasters, D. R.; Kress, M. H.; McNamara, J. M.; Dolling, U. H. The Stereoselective Synthesis of a Potent Thrombin Inhibitor by a Novel P2−P3 Lactone Ring Opening *J. Org. Chem.* **2004**, *69*, 3620−3627.

(8) Prostakov, N. S.; Soldatenkov, A. T.; Kolyadina, N. M.; Obynochnyi, A. A.; Azafluorenes. Synthesis and Conversions. *Russian Chemical Reviews* **1997**, *66*, 121−138.

(9) Plater, M. J.; Kemp, S.; Lattmann, E.; Heterocyclic Free Radicals. Part 1. 4,5-Diazafluorene Derivatives of Koelsch's Free Radical: An EPR and Metal-Ion Complexation Study. *J. Chem. Soc., Perk. Trans. 1* **2000**, 971−979.

(10) Evans, D. A.; Truesdale, L. K.; Carroll, G. L. Cyanosilylation of aldehydes and ketones. A convenient route to cyanohydrin derivatives. *J. Chem. Soc., Chem. Commun.* **1973**, 55.

(11) Grunewald, G. L.; Brouillette, W. J.; Finney, J. A.; Synthesis of α-Hydroxyamides Via the Cyanosilylation of Aromatic Ketones. *Tetrahedron Lett.* **1980**, *21*, 1219−1220.

(12) Mazaleyrat, J.-P.; Wakselman, M.; Formaggio, F.; Crisma, M.; Toniolo, C. Synthesis of terminally protected 9-amino-4,5-diazafluorene-9-carboxylic acid, the first rigid, transition-metal receptor, disubstituted glycine. *Tetrahedron Lett.* **1999**, *40*, 6245−6248.

(13) Comins, D. L.; Stroud, E. D.; Herrick, J. J.; Regioselective Addition of Grignard Reagents to the 1-Phenoxycarbonyl Salts of Alkyl Nicotinates. *Heterocycles* **1984**, *22*, 151.
(14) Epsztajn, J.; Plotka, M. W.; Grabowska, A. Application of organolithium compounds in organic synthesis. Part 19. Synthetic strategies based on aromatic metalation. A concise regiospecific synthesis of 3-halogenated picolinic and isonicotinic acids. *Synth. Commun.* **1997**, *27*, 1075−1086.
(15) DuPriest, M. T.; Schmidt, C. L.; Kuzmich, D.; Williams, S. B.; A Facile Synthesis of 7-Halo-5H-indeno[1,2-b]pyridines and -pyridin-5-ones. *J. Org. Chem.* **1986**, *51*, 2021−2023.
(16) Wang, P.; Layfield, R.; Landon, M.; Mayer, R. J.; Ramage, R.; Transfer active ester condensation: A novel technique for peptide segment coupling. *Tetrahedron Lett.* **1998**, *39*, 8711−8714.
(17) Lewis, S. D.; Ng, A. S.; Baldwin, J. J.; Fusetani, N.; Naylor, A. M.; Shafer, J. A. Inhibition of thrombin and other trypsin-like serine proteases by cyclotheonamide. *Thromb. Res.* **1993**, *70*, 173−190.
(18) Lewis, S. D.; Ng, A. S.; Lyle, E. A.; Mellott, M. J.; Appleby, S. D.; Brady, S. F.; Stauffer, K. J.; Sisko, J. T.; Mao, S. S.; Veber, D. F.; Nutt, R. F.; Lynch, J. J.; Cook, J. J.; Gardell, S. J.; Shafer, J. A. Inhibition of thrombin by peptides containing lysyl-alpha-keto carbonyl derivatives. *Thromb. Haemost.* **1995**, *74*, 1107−1112.
(19) Schumacher, W. A.; Steinbacher, T. E.; Heran, C. L.; Seiler, S. M.; Michel, I. M.; Ogletree, M. L. Comparison of thrombin active site and exosite inhibitors and heparain in experimental models of arterial and venous thrombosis and bleeding. *J. Pharmacol. Exp. Therap.* **1993**, *267*, 1237−1242.

JM049423S